Geoderma 337 (2019) 1105–1115

Contents lists available at ScienceDirect

Geoderma

journal homepage: www.elsevier.com/locate/geoderma

Combined effects of temperature and precipitation on soil organic carbon changes in the uplands of eastern China

Liming Zhang[a,b,c], Qiaofeng Zheng[b], Yaling Liu[d,*], Shaogui Liu[e], Dongsheng Yu[a], Xuezheng Shi[a], Shihe Xing[b], Hanyue Chen[b], Xieyu Fan[b]

[a] State Key Laboratory of Soil and Sustainable Agriculture, Institute of Soil Science, Chinese Academy of Sciences, Nanjing 210008, Jiangsu Province, China
[b] Fujian Provincial Key Laboratory of Soil Environmental Health and Regulation, College of Resources and Environment, Fujian Agriculture and Forestry University, Fuzhou 350002, Fujian Province, China
[c] National Engineering Research Center of Juncao, Fujian Agriculture and Forestry University, Fuzhou 350002, Fujian Province, China
[d] Department of Earth and Environmental Engineering, Columbia University, New York, NY 10027, USA
[e] Station of Agriculture Environmental Monitoring, Yangzhou 225603, Jiangsu Province, China

ARTICLE INFO

Handling Editor: David Laird

Keywords:
Soil organic carbon
Temperature
Precipitation
Combined effect
DeNitrification-DeComposition (DNDC)

ABSTRACT

Temperature and precipitation simultaneously influence the soil organic carbon (SOC) in agroecosystems. While these parameters' individual impacts have been extensively studied, their combined effects remain poorly understood at a regional scale. Thus we conducted this study to quantify the combined influence of temperature and precipitation on the SOC in upland-crop fields of the northern Jiangsu Province in eastern China. This quantification was achieved by using the DeNitrification-DeComposition (DNDC, version 9.5) model with the most detailed upland soil database in China. The model simulations indicated that under a scenario where the air temperature (T) increased by 2 °C (T2) and the precipitation (Prec) simultaneously decreased by 20%, the upland soils in the study region were estimated to a sequestered 39.10 Tg C from 2010 to 2039. Meanwhile, a scenario with T2 and a simultaneous increase in Prec by 20% led to a lower C sequestration of 37.39 Tg C. We found that the respective C sequestration from the combined effects of T and Prec in the above two scenarios was 1.24 (or 2.12) Tg C less compared to the sum of their individual effects. Moreover, if the increase of T changed from 2 °C to 4 °C, and the Prec continued to decrease (or increase) by 20%, the C sequestration was 34.69 (or 33.64) Tg C, which was 3.60 (or 3.82) Tg C lower than the sum of the individual effects. Our analysis of the combined effects of T and Prec on the SOC changes suggested that future warming and Prec changes in this region may cause a decrease in the SOC sequestration, but the upland agroecosystems will still serve as a long-term sink for atmospheric CO_2 due to the high application rates of chemical fertilizer and farmyard manure. Furthermore, the separate and combined effects of temperature and precipitation on the SOC changes in the different upland soil groups varied widely due to the heterogeneity of soil properties, physicochemical conditions and fertilizer practices. This result emphasized the importance of using fine scale soil datasets and the need to understand the intricacies in the soil carbon sequestration potential at a regional scale in a changing climate.

1. Introduction

Recently, global climate change has become an important environmental issue (Enríquez-de-Salamanca et al., 2017). The soil plays a pivotal role in governing the global carbon cycle because of the very large soil organic carbon (SOC) stock, which is 1550 Pg C in terrestrial ecosystems (Batjes, 1996; Meersmans et al., 2011). In general, the role of the SOC as a source or sink depends on the regional temperature and precipitation (Poll et al., 2013). According to the Intergovernmental Panel on Climate Change (IPCC), the average temperature at a global scale will increase by 0.3 to 4.8 °C by the end of this century (IPCC, 2013). Increases in the atmospheric temperature are anticipated to increase the SOC decomposition rates due to the increase in the mineralization of the soil carbon, as well as the soil respiration, especially in upland mineral soils (Davidson and Janssens, 2006; Bond-Lamberty and Thomson, 2010; Álvaro-Fuentes et al., 2012). Some studies show that an increase of 1 °C in the air temperature could cause a 10–28% greater C release (11–34 Pg C $year^{-1}$) (Schimel et al., 1994). Furthermore, precipitation is identified as a main factor that affects the organic C input into the soil (Gabarrón-Galeote et al., 2015). Altered precipitation

* Corresponding author.
E-mail address: yl3937@columbia.edu (Y. Liu).

https://doi.org/10.1016/j.geoderma.2018.11.026
Received 26 March 2018; Received in revised form 5 November 2018; Accepted 12 November 2018
Available online 23 November 2018
0016-7061/

patterns will have a significant impact on the function and structure of terrestrial ecosystems because water is an elemental driver of virtually all chemical and biological processes including plant growth and survival, photosynthesis, microbial activity and soil respiration (Gerten et al., 2008). A meta-analysis of the precipitation manipulation experiments showed that increased precipitation stimulates soil respiration on average by 30%, whereas decreased precipitation reduces soil respiration by 12% (Wu et al., 2011).

Recently, we have witnessed increases in knowledge on the impacts of climate change on the SOC changes. Nonetheless, the current knowledge is mostly from a single climatic factor, such as a warming temperature (T) or a changing precipitation (Prec) (Sakurai et al., 2012; Longbottom et al., 2014; Ghosh et al., 2016; Mureva and Ward, 2017). Despite all of the efforts dedicated to the effects of single climatic factors, applying their individual effects or even linearly summing them up to predict the SOC changes may cause large biases. This finding is observed because in reality, all of the climatic factors act collectively, simultaneously and nonlinearly, rather than separately, to affect the SOC. Therefore, the knowledge of their combined effects is needed for understanding the carbon cycle of terrestrial ecosystems in response to climate change (Zhao et al., 2018). Although there are many other climatic factors, such as radiation, humidity and aerosols, that may also exert appreciable effects on the SOC variations, in this study, we aimed to examine the collective and nonlinear impacts of the two most critical climatic drivers (Prec and T) that have not been thoroughly elucidated to date. This study represents an important step toward a thorough understanding of the fate of the SOC in the context of climate change.

The upland soil in the northern Jiangsu Province drew our attention due to its critical position in the national carbon budget of China. Agroecosystems, account for nearly 10% of the total terrestrial SOC storage and are highly sensitive to global climate change (Smit and Skinner, 2002). Previous studies indicate that soil cultivation and land use change have resulted in a loss of 136 Pg C to the atmosphere since 1750 (Lal, 2004). China possesses 126 million ha of upland-crop fields, accounting for approximately 10% of the world's total (Xie et al., 2007). The upland soil in the northern Jiangsu Province is located in the lower reaches of the Huang-Huai-Hai plain, which produces ~27.5% of the total crop production in China (Lei et al., 2006). It is considered a representative grain production region in China because of its long history of cultivation (Yang et al., 2009). More importantly, the SOC changes in this region account for 10.2% of the annual national carbon sequestration of the upland soils (Zhang et al., 2016) compared with 3.7% of the upland area of China. Thus, despite the relatively small land area in this region, it exemplifies the possible SOC responses to climatic change in an agroecosystem of China.

Considering the complexity of the SOC turnover in agroecosystems, process-based models are good tools for predicting the SOC changes, since the models explain the relationships between the ecological drivers and the environmental factors influencing the SOC changes (Francaviglia et al., 2012). Several biogeochemical process-based models have been developed and deployed in recent years to provide estimates of SOC changes at regional scales (Jenkinson and Rayner, 1977; Smith et al., 1997; Tang et al., 2006; Gottschalk et al., 2012; Goglio et al., 2014; Muñoz-Rojas et al., 2017). Among these models, the DeNitrification–DeComposition (DNDC) model has been widely accepted and is used to understand the complex interactions between soil management, crops, and climate change because DNDC integrates the principle mechanisms governing soil C turnover (Gilhespy et al., 2014). However, most applications of the DNDC model at regional scales have been conducted with town- or county-level databases that are characterized by relatively coarse spatial simulation units, with a resolution of approximately 0.5° × 0.5° (Li et al., 2004; Pathak et al., 2005; Tang et al., 2006; Gao et al., 2014). Previous results on sensitivity analyses of the DNDC model indicate that the representation of the soil properties is a large source of uncertainty for simulating SOC changes under specific management conditions at a regional scale (Li et al., 2004; Pathak et al., 2005). The lack of detailed soil information in coarse-scale maps, such as the representation of soil types and spatial variations in soil types, results in the large uncertainties in the estimates of the SOC changes (Zhang et al., 2018). Thus, using high-resolution soil mapping units is very important for improving the prediction accuracy of the SOC changes by the DNDC model.

Recently, a soil map with high spatial resolution and on a 1:50,000 scale was produced for our study region, which is the upland-crop fields of the northern Jiangsu Province in eastern China (Zhang et al., 2016). This new high-resolution digital soil database provided us with an opportunity to better quantify the SOC changes with the DNDC model. The specific objective of this study was to quantify the SOC changes induced from the concurrent effects of the rising T and changing Prec in the northern Jiangsu Province from 2010 to 2039. Based on recent studies, we hypothesized that the collective nonlinear effects of the Prec and T on the SOC changes were less than the sum of their individual effects.

2. Materials and methods

2.1. Study area

The northern Jiangsu Province (116°21′–120°54′E, 32°43′–35°07′N) (Fig. 1) is located in the lower reaches of the Huang-Huai-Hai plain in China, covering an area of 52,300 km^2 and including five cities: Yancheng, Xuzhou, Huaian, Suqian and Lianyungang. This province is an important grain-production area of China because of its intensified agricultural management (Yang et al., 2009). The climate transitions from warm temperate in the north to a subtropical climate in the south of the region, with a mean temperature, annual rainfall, annual sunshine, and frost-free period of approximately 13 to 16 °C, 800 to 1200 mm, 2000 to 2600 h, and 220 days, respectively. The land-use types in the region mainly consist of the upland crop areas, covering 85% of the total land area (Zhang et al., 2016). The dominant cropping system is a summer maize and a winter wheat rotation.

The upland soils in the region are derived mostly from river alluvium, the Yellow River flood alluvial, loess deposits and fluvio-marine deposits. These soils are classified into 8 soil groups, 22 soil subgroups, 85 soil families and 338 soil species, according to the Genetic Soil Classification of China (GSCC) (Huang et al., 2017). The eight GSCC groups are cross-referenced in the World Reference Base Soil Taxonomy (WRB) system as chloridic solonchaks (saline soil), eutric cambisols (cinnamon soil), haplic luvisols (brown soil), cambisols (purplish soil), eutric acrisols (lime concretion black soil), regosols/leptosols (lithosols soil and limestone soils) and fluvisols (fluvo-aquic soil) (Gray et al., 2011).

2.2. DNDC model and regional simulations

The DNDC (version 9.5) model couples the denitrification and decomposition processes which are influenced by the soil environment to simulate and quantify the long-term carbon and nitrogen cycles in agroecosystems (Gilhespy et al., 2014). The DNDC is recognized as one of the most successful process-based soil models, and it is suitable for application across a wide range of climatic zones and geographic regions (Tonitto et al., 2007; Wang et al., 2008; Abdalla et al., 2011). The DNDC contains six submodels, including soil climate, crop growth, decomposition, nitrification, denitrification and fermentation. A detailed description of this model is found in the literature (Li, 2007a; Gilhespy et al., 2014).

Typically, the DNDC uses county as the basic spatial simulation unit at a regional scale (Li et al., 2004). These simulations may have high spatial uncertainty because the within-county variations of the soil properties are ignored (Zhang et al., 2014). Another drawback of the county-scale model simulations is that the effects of the different crop management practices associated with the different soil types on the

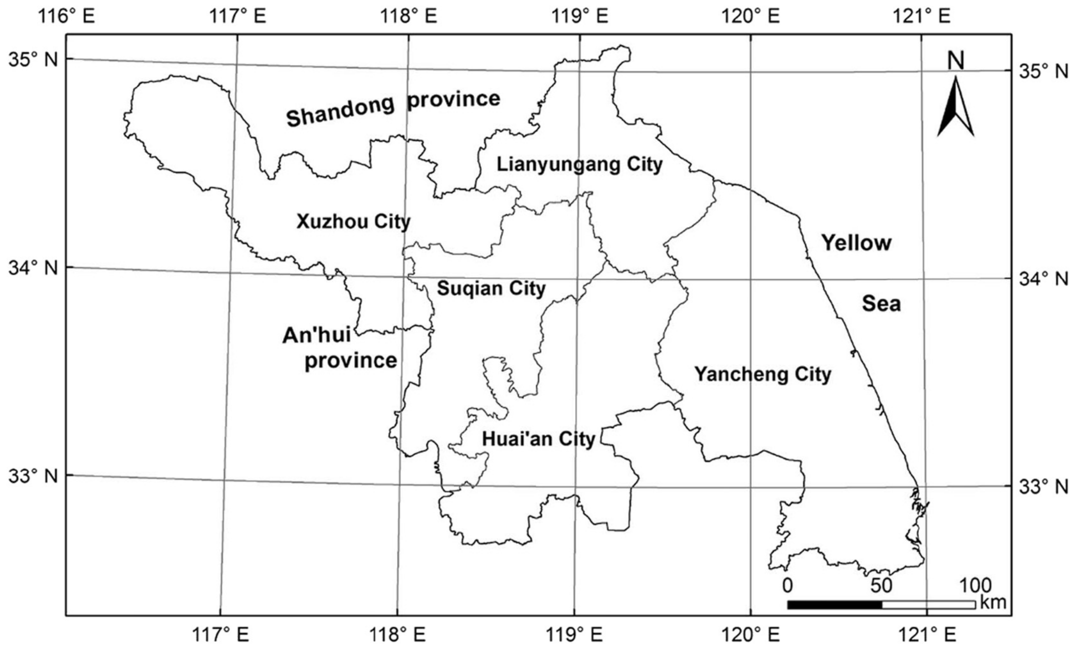

Fig. 1. Geographical map of the northern Jiangsu Province in China.

SOC are ignored at the country level. In this study, we employed the DNDC model using a polygon-based 1:50,000 soil database that well represents the spatial heterogeneity of the soil characteristics, and the polygon was used as the basic simulation unit. The model simulation was done for the upper soil layer (0–50 cm) (Gilhespy et al., 2014).

2.3. Data

An important task for using the DNDC model at a regional scale is to collect adequate input data to run the model. The soil properties, climate, and agricultural management practices for the 29 constituent counties in the study area were collected.

2.3.1. Soil data

The soil database consists of 17,024 polygons. The database was produced by digitizing and recompiling the 29 county-level 1:50,000 field maps. The polygon-specific soil properties were derived from the analyses of 983 upland soil profiles. These soil profiles were collected during the 2nd National Soil Survey of China, which spanned from the 1980s to 1990s and was the most detailed survey of the soil properties in China (Zhi et al., 2014). The soil properties were linked to the soil polygons using the Pedological Knowledge Based (PKB) method based on a GSCC system (Zhao et al., 2006). The PKB method not only considers the match of the soil type between the soil profiles and the map units but also the spatial distance between them. This method links the soil attributes of each profile to their corresponding polygons on the map. The link was determined based on the soil information recorded in the county-level soil series, mainly according to the principle of the similarity and identity in the soil parent materials and soil types and the coexistence or adjacency of the distribution area. For a detailed description and illustration of the PKB method, readers are referred to Zhao et al. (2006). The soil properties in each polygon include the soil name, profile location, thickness of the profile, clay content, bulk density, pH, organic carbon content, etc.

2.3.2. Climate data

The meteorological data from 1980 to 2009 at 7 weather stations in the study area were obtained from the National Meteorological Information Center, at the Chinese Meteorological Administration (China Meteorological Administration, 2011), including the daily precipitation and the maximum and minimum air temperature. For each of the 29 counties, the climate data from the nearest weather station were used (Tang et al., 2006). The most recent 30-year climate data (1980–2009) were used to simulate the baseline climate for 2010–2039 (Xu et al., 2011).

The baseline scenario employed the conventional management practices in 2009 throughout the period of 2010 to 2039. This finding means that the agricultural management practices, including the nitrogen fertilizer application rates, the livestock and agricultural populations, the tillage, the crop residue, and the planting and harvest dates, were assumed to stay the same as that of 2009. Alternative scenarios were compiled by changing T and Prec from those under the baseline scenario. The daily maximum and minimum T from every day were set to increase by 2 °C and 4 °C, respectively. The amount of Prec for every rainfall event was set to increase or decrease by 20%. The details of the baseline and alternative climate scenarios are presented in Table 1. Note that the baseline and alternative climate scenarios used the same soil data and crop management practices.

2.3.3. Farming management data

The cropping dataset included the phenological and physiological parameters (e.g., maximum yield, C/N ratio, biomass partitions, cumulative thermal degree days, and water requirements) for summer maize and winter wheat. More crop parameters for the summer maize and winter wheat rotation systems are found in Li (2007b). The agricultural management dataset included the nitrogen fertilizer application rates, the livestock and agricultural populations, the tillage, the crop residue, and the planting and harvest dates. These data in 2009 were collected at the county level by the Resources and Environmental Scientific Data Center of the Chinese Academy of Sciences.

2.4. DNDC model verification at the field site and regional scale

Our model was validated using 9-year ground measurements from a field site in the northern Jiangsu Province. The soil type at the validation site was fluvo-aquic soil, which was the dominant soil type in the study region and accounted for 52.7% of the total upland soil area according to the 1:50,000 digital soil map. The validation results indicated that the model estimates were encouragingly consistent with the observations. More detailed discussions about the DNDC model

Table 1
Baseline and alternative climate scenarios in the northern Jiangsu Province.

Scenario	Conditions or variations
Baseline (conventional management, CT)	Summer maize-winter wheat rotation, 15% of crop residue was returned to soil annually (0.15R), 20 cm tilling depth for maize and 20 cm for wheat of conventional tillage, manure of 10% of human wastes and 20% of livestock wastes, and initial concentration of CO_2 in the atmosphere was 379 ppm in 2009, later increases at 1.9 ppm year^{-1}.
	Alternative climate scenarios
Air temperature	Increase the max and min temperature of every day in the baseline data base by 2 °C and 4 °C (T2 and T4, respectively)
Precipitation	Increase (I2)/decrease (D2) the amount of precipitation for every rainfall event by 20%.
Combined scenarios of the temperature and precipitation	Increase the max and min temperature of every day in the baseline data base by 2 °C, and simultaneously decrease (T2D2) or increase (T2I2) the amount of precipitation for every rainfall event by 20%.
	Increase the max and min temperature of every day in the baseline data base by 4 °C, and simultaneously decrease (T4D2) or increase (T4I2) the amount of precipitation for every rainfall event by 20%.

validation for this region are found in Zhang et al. (2016).

Previous studies suggest most dynamic models have not yet been validated by regional scale data. Thus, there are concerns about their accuracy when they are applied to larger area SOC simulations (Shi et al., 2010). This study compares the simulation results with the spatial distribution of the SOC measurements from 1152 upland soil sampling sites acquired in 2008, which was sponsored by the Ministry of Agriculture of the People's Republic of China (Fig. 2).

Four statistical metrics, including the root mean square error (RMSE) (Loague and Green, 1991), mean absolute error (MAE) (Kumar, 2015), relative error (E) (Whitmore et al., 1997), and correlation coefficient (r) (Gollany and Elnaggar, 2017) were used to measure the differences between the observed and model predicted SOC values at a regional scale. The RMSE, MAE and E were defined as:

$$\mathrm{RMSE} = \sqrt{\frac{1}{n}\sum_{i=1}^{n}(V_{oi} - V_{pi})^2} \tag{1}$$

$$MAE = \frac{1}{n}\sum_{i=1}^{n} ABS(V_{oi} - V_{pi}) \tag{2}$$

$$E = \frac{100}{n} \times \sum_{i=1}^{n} \frac{V_{oi} - V_{pi}}{V_{oi}} \tag{3}$$

where V_{oi} are the measured values, V_{pi} are the simulated values, and n is total 1152 number in the sequence of the measured and simulated data pairs. The greater r value and the smaller RMSE or MAE value suggests the better agreement between the model-predicted and measured SOC values. If E is < 5% or between 5% and 10%, the modeling is satisfactory or acceptable, respectively; otherwise, it is unacceptable (Whitmore et al., 1997).

2.5. Data comparison and analysis

The annual average SOC change (AASC, kg C ha^{-1} year^{-1}) represented the aggregated long-term annual average change in the SOC for the region or soil group. The total SOC change (TSC, Tg C) was the accumulated SOC change during the study period for the region or soil group.

The uncertainty in SOC estimation was partially attributed to the variability of the soil properties used as inputs into the model or in the estimation process (Grosz et al., 2017). To further quantify the impact of the soil properties on the regional estimation of the SOC changes, the correlation between the soil properties and AASC was analyzed. The Pearson's test and a multiple stepwise regression analysis were performed using the Statistical Package for Social Sciences (SPSS) statistical software (Leech et al., 2008; Saint-Laurent et al., 2014).

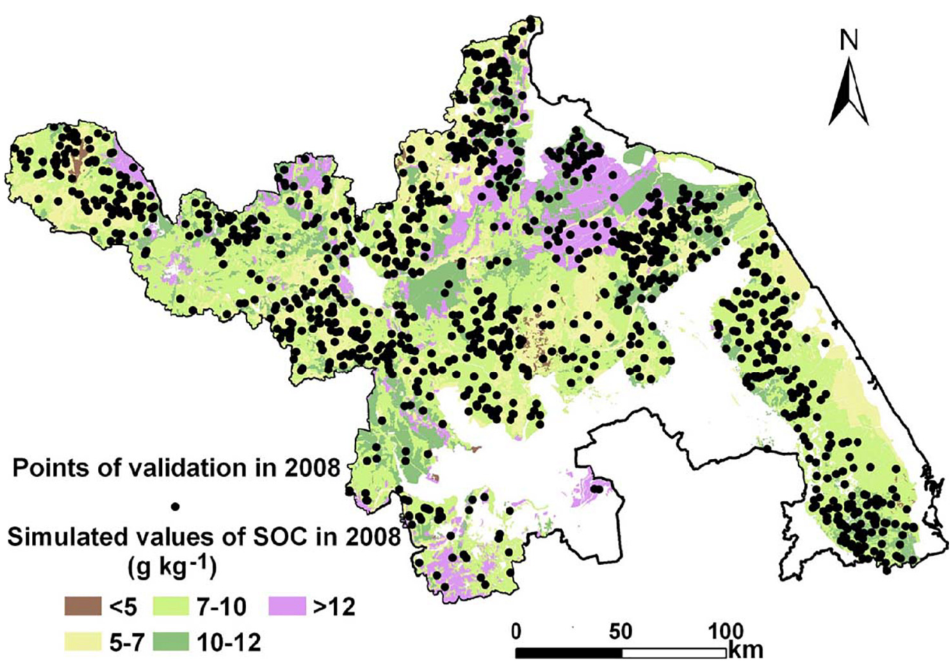

Fig. 2. Spatial distribution of validation points and simulated SOC values from the 1:50,000 soil database for the study region for 2008.

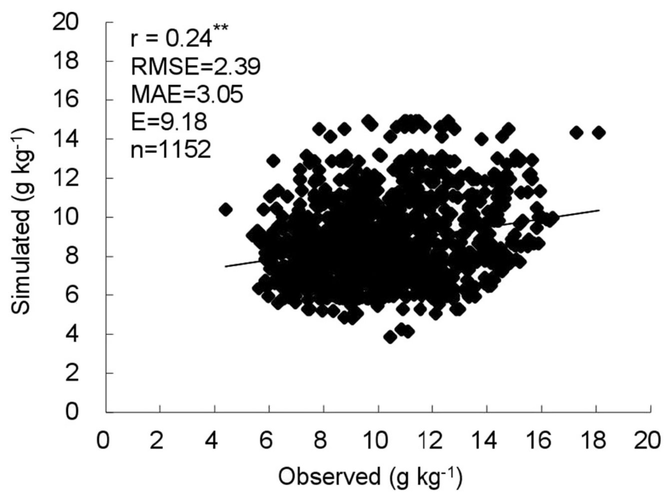

Fig. 3. Comparison between the observed SOC and simulated values from the 1:50,000 soil database of the study region for 2008.

3. Results and discussion

3.1. Evaluation of the DNDC model

A map of the SOC content for the upland soils at the top layer (0–20 cm) in the northern Jiangsu Province in 2008 was constructed on the basis of the simulated data from the 1:50,000 soil databases (Fig. 2). The DNDC simulated SOC content for the 1152 upland soil sampling sites in 2008 varied from 3.9 g kg^{-1} to 15 g kg^{-1} (Fig. 2), which was similar to their observational range of 4.4 g kg^{-1} to 18 g kg^{-1}. Specifically, 99.7% of the simulated values for the upland soil samples were within the observational range. Furthermore, Fig. 3 depicts that the simple correlation coefficient (r) between the observed and measured SOC levels was 0.24 ($p < 0.01$). The relative error (E) was 9.18%, within the range of 5%–10%, which demonstrated that the DNDC model was acceptable for modeling the SOC of the study region (Whitmore et al., 1997). Likewise, the low values of the RMSE (2.39 g kg^{-1}) and MAE (3.05 g kg^{-1}) indicated an encouraging model performance (Fig. 3).

3.2. Annual variations in the SOC in the northern Jiangsu Province

The SOC generally increased from 2010 to 2039 over the study region (Figs. 4 and 5). Under the conventional management scenario (CT), the SOC stocks (SOCD) in the upland soils of the study area were predicted to increase from 28.22 Mg C ha^{-1} in 2010 to 37.02 Mg C ha^{-1} in 2039 (Fig. 5). Consequently, the TSC reached 41.76 Tg C in the topsoil layer (0–50 cm) in the region for the period of 2010 to 2039 with an AASC of 355 kg C ha^{-1} $year^{-1}$. These results were consistent with results from other studies. Yu et al. (2006) found that the SOC of fluvo-aquic soils and brown soils in the Huang-Huai-Hai plain obviously increased during the periods of 1980 to 2000, and the increased rates reached 19% and 14%, respectively. Pan et al. (2010) found that the annual average SOC change of China's upland soils was 56 ± 200 kg C ha^{-1} $year^{-1}$ from 1985 to 2006. Liao et al. (2009) found that the average topsoil SOC content (0–20 cm) in the Jiangsu Province increased from 9.45 g kg^{-1} in 1982 to 10.9 g kg^{-1} in 2004, based on 662,690 and 24,167 measured samples in 1982 and 2004, respectively. This C sequestration is mainly attributed to the current management practices in this region. A high rate in fertilizer use (492 kg N ha^{-1} $year^{-1}$) and farmyard manure application (17.27 kg N ha^{-1} $year^{-1}$) and the return of crop residue to the soils in this region likely increase the SOC (Zhang et al., 2016) (Table 2). Adding fertilizer usually results in an increased biomass production in the roots and stubble from the increasing yields (Singh and Lal, 2005). Therefore, it may increase the C sequestration in the soils. Additionally, the application of organic manure not only increases the overall input of the organic carbon into the soil but also enhances the microbial activity (Qi et al., 2016). This, in turn, controls the rate of C input relative to C export and accelerates the plant residue deposition by the increasing the plant net primary productivity. Furthermore, the correlation coefficients (Pearson's test) between the average annual SOC change and soil properties showed that all the variables (i.e., initial SOC content, pH, bulk density, and clay content) had significant effects ($p < 0.01$) on the AASC (Table 3). In particular, the clay content and the initial SOC content were the two most dominant parameters controlling the C accumulation among all of the main soil properties according to the stepwise linear regression (Table 4). The clay content and initial SOC value accounted for 60% of the variation in the average annual SOC change for the upland soils from 2010 to 2039, while the other soil parameters only accounted for 4.4%. The relatively high clay (28%) and low initial SOC (6.0 g kg^{-1}) in the upland soils in this region (Table 2) facilitate the SOC accumulation (Six et al., 2002). Our findings are consistent with many previous studies, which indicate that China's croplands will maintain a high rate of C sequestration in the next 40 years, even if the agricultural management practices remain at the current levels (Yu et al., 2013).

As seen in Fig. 5, the TSC from 2010 to 2039 varied under different climate change scenarios, including 38.35 Tg C if the T increased by 2 °C (T2), 42.33 Tg C if the Prec decreased by 20% (D2), and 40.67 Tg C if the Prec increased by 20% (I2). The region-level AASC were 326 and 345 kg C ha^{-1} $year^{-1}$ for the T2 and I2 scenarios, which were 8.15% and 2.61% lower than the baseline scenario, respectively. Our results showed that the decomposition of the SOC was more sensitive to temperature change than precipitation. These results are consistent with previous studies (Guntiñas et al., 2013; Karhu et al., 2014), in which the temperature played a major role in the reduction of the SOC. A large number of studies find that the microbial activities and processes, for example, the substrate uptake, growth, and respiration, are dependent on temperature (Conant et al., 2011; Royles et al., 2013; Streit et al., 2014). Thus, the SOC decomposition could be sensitive to increasing temperature and the SOC would decay faster in the warmer environment (Zhang et al., 2015). We also found that the rate of the sequestration of C was slower with higher temperatures in this region. This finding was observed primarily because the rising T affected the microbial activity, and microbes tend to consume labile organic carbon fractions as an energy source, which results in a higher soil respiration, reducing the amount of carbon retained in the soil (Gaumont-Guay et al., 2006; Bond-Lamberty and Thomson, 2010; Lefèvre et al., 2014). Recent results from a long-term soil warming study indicate that the structural and functional changes in the microbial community are the dominant factor controlling the decomposition of soil C under warming conditions (Melillo et al., 2017). In particular, significant changes in the microbial community occur after an increase in temperature by larger than ~2 °C (Zou et al., 2018). Thus, the temperature sensitivity of the SOC strongly regulates the C balance of terrestrial ecosystems in a warming climate.

Comparing with the baseline scenario, the I2 scenario showed a slight decrease in the average annual SOC by ~10 kg C ha^{-1} $year^{-1}$ during the period of 2010 to 2039 in this region (Fig. 5). The findings were broadly consistent with those of Arunrat et al. (2018), who found that an increasing Prec resulted in a loss of SOC sequestration at all the survey sites of soil nutrient status by 30.0%, 27.1%, 21.1%, and 18.6% under an RCP (Representative Concentration Pathway) 8.5, RCP6.0, RCP4.5, and RCP2.6, respectively in the Roi Et Province, Northeast Thailand. The northern Jiangsu Province is located in a transitional climate zone that ranges from warm temperate to a subtropical climate, which has a high mean annual rainfall (> 900 mm) (Table 2). Excessive water from heavy rainfall events leads to a decrease in crop biomass due to the leaching of nitrogen from the first soil layer to the deeper

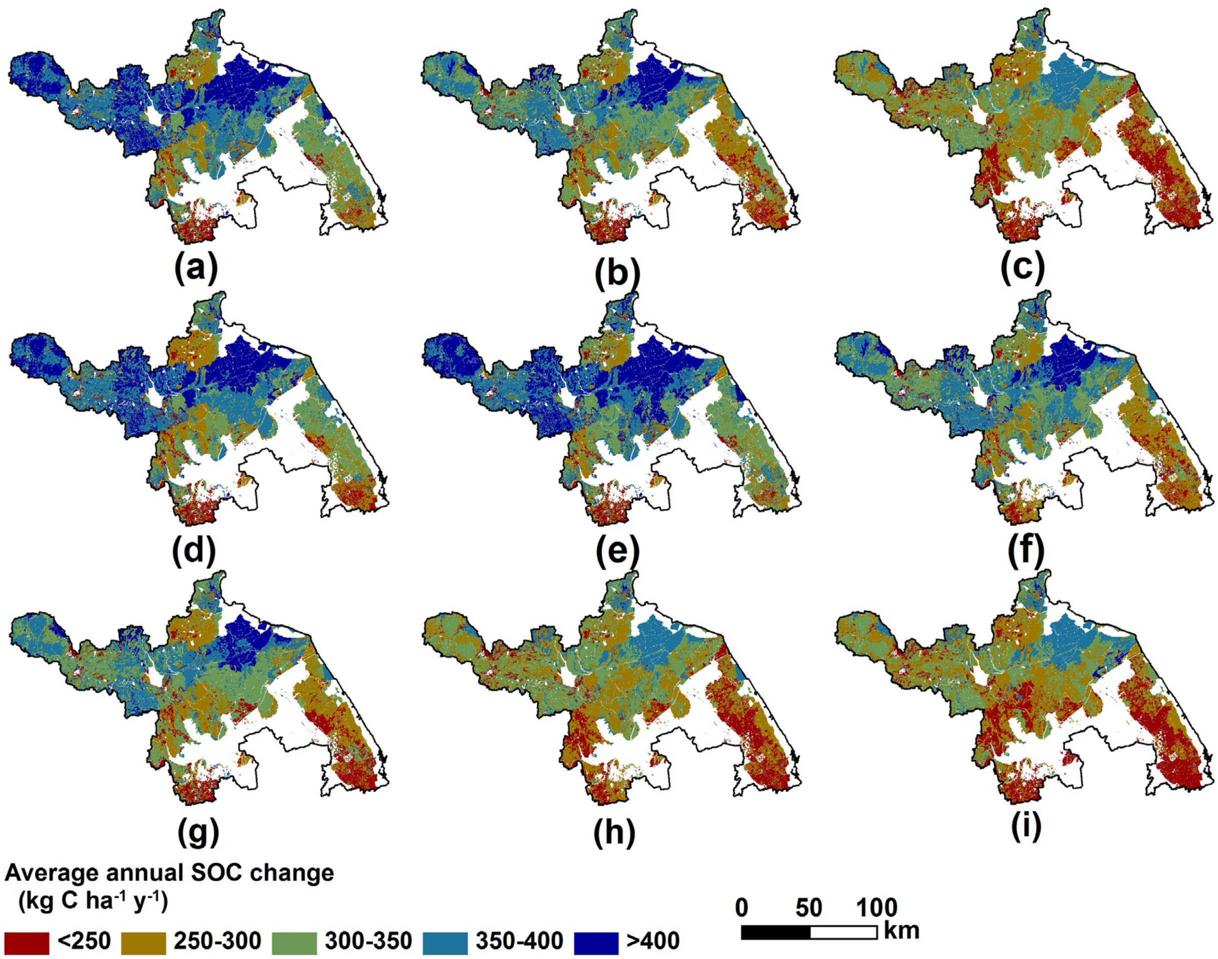

Fig. 4. Spatial patterns of polygon-level average annual SOC change under the baseline and alternative climate scenarios from 2010 to 2039: (a) conventional management (baseline); (b) increase in air temperature by 2 °C (T2); (c) increase in air temperature by 4 °C (T4); (d) decrease in precipitation by 20% (D2); (e) increase in precipitation by 20% (I2); (f) increase in air temperature by 2 °C, and simultaneously decrease in precipitation by 20% (T2D2); (g) increase in air temperature by 2 °C, and simultaneous increase in precipitation by 20% (T2I2); (h) increase in air temperature by 4 °C, and simultaneous decrease in precipitation by 20% (T4D2); and (i) increase in air temperature by 4 °C, and simultaneous increase in precipitation by 20% (T4I2).

layers (Peinetti et al., 2008). Consequently, this causes a decrease in the SOC content as a result of the reduced returns of the crop residues to the soil. On the other hand, our work indicated that an increasing Prec leads to an accelerated decomposition of the SOC, as a result of rising precipitation-increased microbial activity (Alvarez and Alvarez, 2001). This phenomenon was consistent with the study of Meier and Leuschner (2010), who found that the SOC decreased by approximately 25% with an annual Prec > 900 mm $year^{-1}$ relative to those with a Prec < 600 mm $year^{-1}$. In contrast, the AASC was 359 kg C ha^{-1} $year^{-1}$ for the D2 scenario, which was 1.37% higher than the baseline scenario. This was possibly due to the limitation of the microbial activities caused by the decreased soil moisture (Liu et al., 2016), or the decreased autotrophic respiration under low soil water availability (Sardans et al., 2008).

The soil C sequestration induced from the combined effects of the temperature and precipitation changes was less than from the sum of their individual effects (Fig. 5a), which validated our hypothesis. Nevertheless, this area will continue to serve as a carbon sink (Figs. 4 and 5). The AASC values were 332 and 318 kg C ha^{-1} $year^{-1}$ for the T2D2 (T increase 2 °C and Prec decrease 20%) and T2I2 (T increase 2 °C and Prec increase 20%) scenarios, which were 3.07% and 5.36% lower than their sum of the individual T and Prec effects, respectively. This finding is observed because the effects of the warming and precipitation manipulation on the soil temperature and moisture are not independent, but rather show interactive effects (Li et al., 2017). The T2D2 yielded a lower AASC relative to the sum induced from their individual effects, and this was because the combined effects of T2 and D2 cause a decrease in the Net Primary Productivity (NPP), which may lead to a decrease in the organic matter input (Dintwe and Okin, 2018). Meanwhile, in the T2I2 scenario, the lower AASC relative to the sum of their individual effects was observed because the microbial activity tends to be higher in a warmer and wetter climate, which results in a reduction in C sequestration (Yang et al., 2011). Overall, our modeling study revealed nonlinear patterns in the SOC changes in response to the global change factors and suggested that the effects of the combined climate anomalies should be considered when designing scenarios of climate change to predict ecosystem responses and in setting up new experiments (Zhou et al., 2008).

The SOC content was very sensitive to the temperature changes (Fig. 5). When the T increased by 4 °C, and simultaneously the P decreased (T4D2) or increased (T4I2) by 20%, after 30 years of CT management the estimated TSC values in 2039 were 34.69 or 33.64 Tg C, respectively, which was 9.40% and 10.2% lower than the sum of the TSC induced from the individual effects of the T or Prec. The corresponding AASC values were 295 or 286 kg C ha^{-1} $year^{-1}$, respectively (Fig. 5a). Our findings suggested that the C sequestration rate was slower with higher temperatures in this region. Nonetheless, it is important to note that the upland soils in this region continued to be a long-term sink for atmospheric CO_2 under the changing T and Prec, even if the T increased by 4 °C (Figs. 4 and 5).

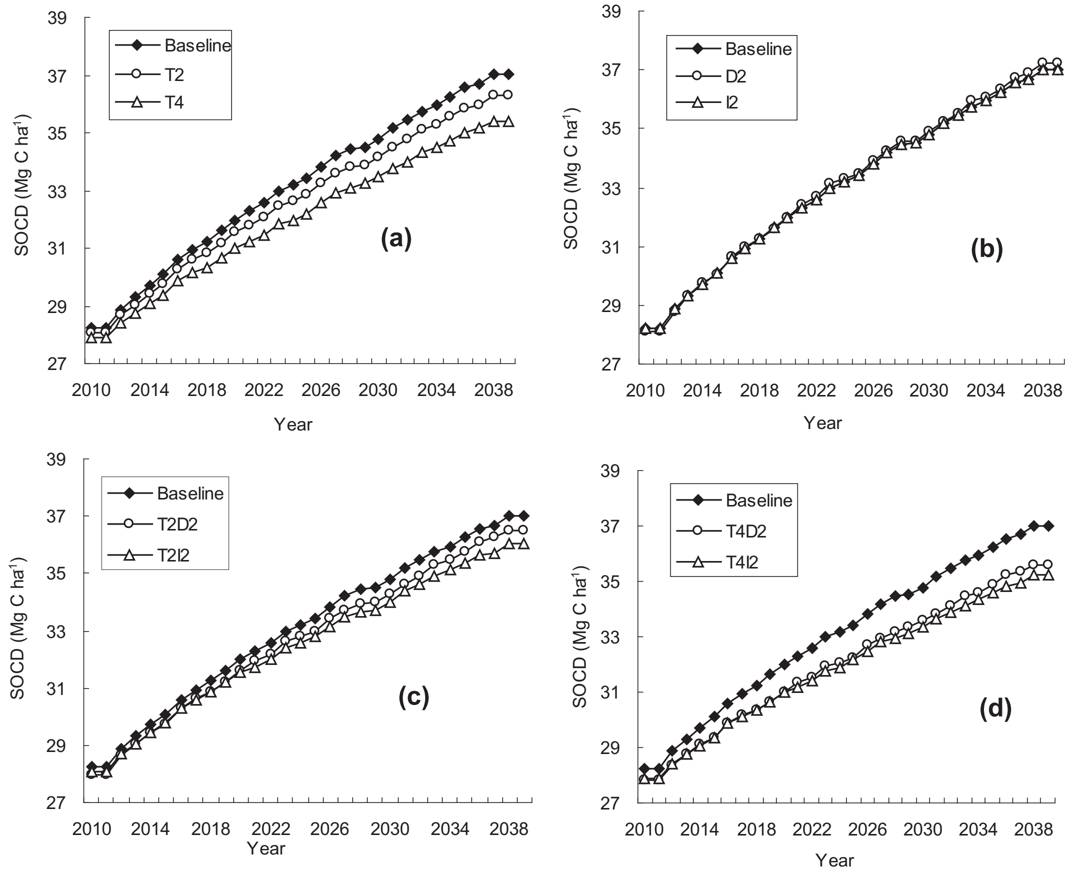

Fig. 5. Annual SOC density (SOCD) from 2010 to 2039 under baseline and alternative climate scenarios: (a) baseline–conventional management; T2 and T4–increase in air temperature by 2 °C and 4 °C, respectively; (b) baseline–conventional management; D2 and I2–decrease and increase in precipitation by 20%, respectively; (c) baseline–conventional management; T2D2 and T2I2–increase in air temperature by 2 °C, and simultaneous decrease and increase in the precipitation by 20%, respectively; (d) baseline–conventional management; T4D2 and T4I2– increase in air temperature by 4 °C, and simultaneous decrease and increase in precipitation by 20%, respectively.

3.3. Comparison of the SOC changes among the different upland soil groups

The SOC variation is the result of the long-term net balance between the loss and accumulation of the SOC in the soil and is largely determined by the soil types (Singh et al., 2011; Labaz et al., 2014). Under a similar climate, the microbial decomposition processes are significantly different among soil types because of distinct microbial enzyme activities and community structures as a result of specific soil conditions, leading to soil-dependent stabilization/destabilization of the SOC (Luo et al., 2017). Thus, the separate or combined effects of the T and Prec, on the potential soil C sequestration, were greatly influenced by the soil type (Table 5).

The group of fluvo-aquic soils accounted for 53% of the total upland soil area in the study area. The modeled AASC from the fluvo-aquic soil group had the highest C-sequestration rate among all the soil groups in most scenarios, ranging from 296 to 378 kg C ha^{-1} year^{-1} (Table 5).

Table 2
The model input of climatic factors and the fertilizer-use rate for the entire study area and different upland soil groups under the baseline scenario.

	Areas 10^4 ha	Climatic factors		Fertilizer amount		Soil properties			
		Mean annual temperature (°C)	Annual mean rainfall (mm)	Manure (kg N ha^{-1} year^{-1})	Fertilizer (kg N ha^{-1} year^{-1})	Clay (%)	Initial SOC (g kg^{-1})	Bulk density (g cm^{-3})	pH
Whole northern Jiangsu Province									
Northern Jiangsu Province	393	14.7	948	17.27	492	28	6.0	1.31	8.0
Soil groups									
Fluvo-aquic soil	207	14.7	918	17.83	517	26	5.55	1.31	8.2
Saline soil	95	14.6	1010	15.68	538	29	6.51	1.28	8.3
Lime concretion black soil	32	14.6	942	18.90	434	41	8.23	1.29	7.7
Brown soil	29	14.3	938	19.76	347	18	4.53	1.44	6.7
Cinnamon soil	22	15.1	947	14.40	409	36	5.93	1.33	8.0
Lithosols soil	5.8	15.4	1048	13.08	265	38	9.16	1.29	7.3
Purplish soil	1.1	14.1	912	19.92	437	14	4.27	1.38	7.5
Limestone soil	0.72	15.4	1048	13.08	265	40	9.39	1.35	7.1

The value of all factors is weighted average by the area of each polygon.

Table 3
Correlation coefficients (Pearson's test) between the average annual SOC change and soil properties under the baseline and alternative climate scenarios.

	Number of polygons	Clay (%)	Initial SOC (g kg^{-1})	Bulk density (g cm^{-3})	pH
Natural range of each soil properties	17,024				
Soil properties		0.10–82	0.35–22.5	0.69–1.87	5.6–9.6
Baseline					
Baseline		0.24**	−0.54**	−0.19**	0.16**
Alternative climate scenarios					
T2		0.26**	−0.53**	−0.17**	0.082**
T4		0.24**	−0.55**	−0.13**	−0.013
I2		−0.48**	0.31**	−0.22**	0.14**
D2		0.20**	−0.56**	−0.17**	0.13**
T2D2		0.24**	−0.54**	−0.15**	0.065**
T2I2		0.32**	−0.48**	−0.20**	0.072**
T4D2		0.22**	−0.56**	−0.12**	−0.031**
T4I2		0.31**	−0.51**	−0.17**	−0.030**

Baseline–conventional management; T2 and T4–increase air temperature by 2 °C and 4 °C, respectively; D2 and I2–decrease and increase precipitation by 20%, respectively; T2D2-increase the air temperature by 2 °C, and simultaneously decrease the precipitation by 20%; T2I2-increase the air temperature by 2 °C, and simultaneously increase the precipitation by 20%; T4D2-increase the air temperature by 4 °C, and simultaneously decrease the precipitation by 20%; T4I2-increase the air temperature by 4 °C, and simultaneously increase the precipitation by 20%.

** Significant at the 0.01 level.

Table 4
Variation in the average annual SOC change (AASC) contributed from soil properties under the baseline and alternative climate scenarios.

Scenario	Number of simulation units	ΔR^2 [a]				Adjusted R^2
		Clay (%)	Initial SOC (g kg^{-1})	Bulk density (g cm^{-3})	pH	
Baseline	17,024	0.31***	0.29***	0.034***	0.011***	0.64***
Alternative climate scenarios						
T2		0.33***	0.28***	0.025***	0.0010***	0.64***
T4		0.33***	0.31***	0.016***	0.0030***	0.65***
I2		0.23***	0.37***	0.040***	0.010***	0.64***
D2		0.31***	0.27***	0.033***	0.0060***	0.63***
T2D2		0.32***	0.29***	0.020***	0.0010***	0.63***
T2I2		0.39***	0.23***	0.030***	0.0010***	0.66***
T4D2		0.30***	0.32***	0.014***	0.0060***	0.64***
T4I2		0.39***	0.26***	0.021***	0.0050***	0.68***

Baseline–conventional management; T2 and T4–increase air temperature by 2 °C and 4 °C, respectively; D2 and I2–decrease and increase precipitation by 20%, respectively; T2D2-increase the air temperature by 2 °C, and simultaneously decrease the precipitation by 20%; T2I2-increase the air temperature by 2 °C, and simultaneously increase the precipitation by 20%; T4D2-increase the air temperature by 4 °C, and simultaneously decrease the precipitation by 20%; T4I2-increase the air temperature by 4 °C, and simultaneously increase the precipitation by 20%.

*** Significant at 0.001 probability level.

[a] The change in the R^2 statistic is produced by adding a soil property into stepwise multiple regressions.

Table 5
The **a**verage **a**nnual **S**OC **c**hange (**AASC**, kg C ha^{-1} $year^{-1}$) and the **t**otal **S**OC **c**hange (**TSC**, Tg C) in different soil groups under the baseline and alternative climate scenarios.

Scenario	Fluvo-aquic soil		Saline soil		Lime concretion black soil		Brown soil		Cinnamon soil		Lithosols soil		Purplish soil		Limestone soil	
	AASC	TSC	AASC	TSC	AASC	TSC	AASC	TSC	AASC	TSC	AASC	TSC	AASC	TSC	AASC	TSC
Baseline	372	23.10	345	9.86	333	3.19	324	2.79	345	2.29	210	0.36	367	0.12	175	0.038
Alternative climate scenarios																
T2	340	21.12	311	8.90	314	3.01	313	2.69	321	2.13	209	0.36	339	0.11	173	0.040
T4	302	18.74	274	7.84	289	2.76	295	2.54	282	1.87	203	0.35	308	0.10	157	0.034
I2	362	22.47	335	9.58	331	3.17	309	2.66	342	2.27	211	0.37	352	0.12	176	0.040
D2	378	23.46	347	9.93	335	3.21	338	2.91	346	2.30	210	0.36	373	0.12	175	0.040
T2D2	347	21.50	314	8.98	323	3.09	325	2.80	335	2.22	208	0.036	346	0.11	176	0.038
T2I2	331	20.53	303	8.67	311	2.98	300	2.58	319	2.12	211	0.037	325	0.10	174	0.037
T4D2	306	19.00	276	7.91	292	2.79	305	2.63	282	1.88	203	0.353	311	0.10	157	0.0034
T4I2	296	18.34	271	7.76	286	2.74	285	2.45	281	1.87	204	0.354	298	0.096	158	0.0034

The value of AASC is weighted average by the area of each polygon.
Baseline–conventional management; T2 and T4–increasing air temperature by 2 °C and 4 °C, respectively; D2 and I2–decreasing and increasing precipitation by 20%, respectively; T2D2-increase the air temperature by 2 °C, and simultaneously decrease the precipitation by 20%; T2I2-increase the air temperature by 2 °C, and simultaneously increase the precipitation by 20%; T4D2-increase the air temperature by 4 °C, and simultaneously decrease the precipitation by 20%; T4I2-increase the air temperature by 4 °C, and simultaneously increase the precipitation by 20%.

Among all the soil factors, the stepwise regression models indicated that the clay content, the initial SOC, and the initial soil C content may affect the SOC sequestration rates (Table 1S). The clay content accounted for 27–40% of the variations in the average annual SOC change for the upland soils from 2010 to 2039, and the initial SOC content accounted for 16–29% of the variations. While the organic carbon content in the soil depends on the soil texture, the decomposition rate of the soil carbon is slower in the fine texture soil (clay soil) than the coarse texture soil (Azlan et al., 2012), and soils with a lower initial SOC display a greater SOC increase in the early stages following cultivation (Zhao et al., 2013). As a result, fluvo-aquic soils that possess a relatively high clay (26%) and a low initial SOC (5.55 $g\,kg^{-1}$) (Table 2) have a large potential for carbon sequestration. Furthermore, the average chemical fertilizer application rate in this soil group was relatively high among all the soil groups (Table 2), which increased the SOC levels linearly by the enhancing residue accumulation (Shahid et al., 2017).

The cinnamon soils and lime concretion black soils accounted for 5.6% and 8.1% of the total upland soil area in the northern Jiangsu Province, respectively (Table 2). The modeled AASC under the different scenarios in the period of 2010 to 2039 ranged from 281 to 346 $kg\,C\,ha^{-1}\,year^{-1}$ in the cinnamon soils and from 286 to 335 $kg\,C\,ha^{-1}\,year^{-1}$ in the lime concretion black soils, which was lower than that of the fluvo-aquic soil. This finding was likely observed because those two upland soil groups possessed a high clay content, as well as a low initial SOC content (in cinnamon soils) (Azlan et al., 2012; Zhao et al., 2013) (Table 2).

The saline soils accounted for 24% of the total upland soil area in the study region (Table 2). Their soils' modeled AASC from 2010 to 2039 under the different scenarios ranged from 271 to 347 $kg\,C\,ha^{-1}\,year^{-1}$ (Table 5), which was higher than that of lithosols soil and limestone soil. The main reason was that this upland soil group possessed the highest N-fertilizer application rate among all of the soil groups and presented an alkaline pH (Table 2). Applications of N-fertilizer lead to an increased crop yield and, thus, result in a high rate of organic matter return to the soil (Singh and Lal, 2005), and soils with an alkaline pH produce an unfavorable environment for microbial growth (Pacey and DeGier, 1986), thereby benefitting SOC sequestration.

The purplish soils and brown soils accounted for 0.27% and 7.3% of the total upland soil area in the study region, respectively (Table 2). High C-sequestration rates occurred in these two upland soil groups due to the relatively low initial SOC content and the low initial Prec and T values (Table 2). Soils with lower initial Prec and T values presented lower microbial respiration. This was possibly because of the associated lower soil moisture and soil temperature limited microbial activities (Zhao et al., 2018). Moreover, the application of organic manure in the purplish soil group was as high as 19.2 $kg\,N\,ha^{-1}\,year^{-1}$ (Table 2), and as a result, the total soil carbon content was enhanced.

In contrast to the other groups, limestone soils and lithosols soils accounted for only 0.18% and 1.5% of the total upland soil areas, respectively (Table 2), and they had relatively low SOC sequestration levels (Table 5). The main reason was that these two upland soil groups had a high initial SOC content, high initial Prec and T values, and low N-fertilizer application rates (Table 2). Soils with a higher SOC content and high initial Prec and T values provide a better living environment for microbes, which facilitates microbial decomposition and thus may result in a low SOC sequestration (Li et al., 2004).

The above analysis indicated that the differences in the SOC change among the soil groups resulted either from the soil properties affecting the C-decomposition rate, or from the climate factors affecting the biomass (Ahirwal and Maiti, 2017). The C-sequestration potentials varied substantially from soil group to soil group. This finding suggests that it is necessary to tailor suitable management practices for different soil groups under future global climate change in order to efficiently sequester C without compromising the crop yields or agroecosystem sustainability.

3.4. SOC simulation uncertainties

The first limitation of this work was related to the county-level agricultural management data (Li et al., 2004; Tang et al., 2006; Xu et al., 2011). The data assumed uniform management practices and cropping systems within a county, which ignored the within-county variations (e.g., changes in fertilizer application and crop residue incorporation rates) and thus will inevitably result in bias in the SOC estimates. Therefore, spatially explicit data for agricultural management at a finer resolution (i.e., field level) is particularly needed to improve the accuracy of the DNDC simulations in future research.

The second possible source of the modeling uncertainty was the assumption of a 15% of aboveground crop residue returning to the soil across the whole northern Jiangsu Province during the periods of 2010 to 2039. The fraction of 15% was the national average derived from the Agricultural Ministry (Tang et al., 2006). However, in fact, the fraction had considerable variations among the different counties, which may result in, potentially, large estimation errors.

Another source of uncertainty arises from the static management practice. Management decisions may vary with time, depending on interannual climate changes (Aurbacher et al., 2013), but static agricultural management data were used in this study due to data unavailability. This may cause possible discrepancies from reality.

4. Conclusions

Based on the most detailed and up-to-date 1:50,000 soil database, this study quantified the SOC changes induced by the simultaneous effects of the increasing temperatures and changing precipitation in upland-crop fields in the northern Jiangsu Province of eastern China using the DNDC model. The model simulations indicated that the combined effects of the increased air temperature and simultaneous decrease (or increase) in the precipitation on the C sequestration rate were less than the sum of their individual effects. When the T increased by 2 °C and the precipitation simultaneously decreased or increased by 20%, the C sequestration rates were projected to be 332 or 318 $kg\,C\,ha^{-1}\,year^{-1}$ from 2010 to 2039, respectively, which were 3.07% or 5.36% lower than the sum of the individual T or Prec effects. Similarly, if the T increase changed from 2 °C to 4 °C, with the P still decreased (or increased) by 20%, the C sequestration rates were predicted to be 295 or 286 $kg\,C\,ha^{-1}\,year^{-1}$ from 2010 to 2039, respectively, which were 9.40% or 10.2% lower than the sum of their individual effects. Additionally, the combined effects of the temperature and precipitation on the SOC changes in the different upland soil groups varied widely due to the heterogeneities in the soil properties, physicochemical conditions and fertilizer applications. Our modeling study indicated nonlinear patterns of the SOC changes in response to individual and simultaneous global changes in the study region. The study provides comprehensive possible future scenarios of soil carbon sequestration in the region, which enhances the understanding in the fate of the SOC in the context of climate change.

Supplementary data to this article can be found online at https://doi.org/10.1016/j.geoderma.2018.11.026.

Acknowledgements

This study is supported by the Research Fund of State Key Laboratory of Soil and Sustainable Agriculture, Nanjing Institute of Soil Science, Chinese Academy of Sciences (No. Y20160006), China Postdoctoral Science Foundation (No. 2017M612109), and the Collaborative Innovation for Juncao Ecology Industry of China (No. YK80ND8002). We also acknowledge Professor Changsheng Li (University of New Hampshire, USA) for his valuable help on use of the DNDC model in past years.

References

Abdalla, M., Kumar, S., Jones, M., Burke, J., Williams, M., 2011. Testing DNDC model for simulating soil respiration and assessing the effects of climate change on the CO_2 gas flux from Irish agriculture. Glob. Planet. Chang. 78, 106–115.

Ahirwal, J., Maiti, S.K., 2017. Assessment of carbon sequestration potential of revegetated coal mine overburden dumps: a chronosequence study from dry tropical climate. J. Environ. Manag. 201, 369–377.

Alvarez, R., Alvarez, C.R., 2001. Temperature regulation of soil carbon dioxide production in the humid pampa of Argentina: estimation of carbon fluxes under climate change. Biol. Fertil. Soils 34, 282–285.

Álvaro-Fuentes, J., Easter, M., Paustian, K., 2012. Climate change effects on organic carbon storage in agricultural soils of northeastern Spain. Agric. Ecosyst. Environ. 155, 87–94.

Arunrat, N., Pumijumnong, N., Hatano, R., 2018. Predicting local-scale impact of climate change on rice yield and soil organic carbon sequestration: a case study in Roi Et Province, Northeast Thailand. Agric. Syst. 164, 58–70.

Aurbacher, J., Parker, P.S., Calberto Sánchez, G.A., Steinbach, J., Reinmuth, E., Ingwersen, J., Dabbert, S., 2013. Influence of climate change on short term management of field crops – a modelling approach. Agric. Syst. 119, 44–57.

Azlan, A., Aweng, E.R., Ibrahim, C.O., Noorhaidah, A., 2012. Correlation between soil organic matter, total organic matter and water content with climate and depths of soil at different land use in Kelantan, Malaysia. J. Appl. Sci. Environ. Manag. 16, 353–358.

Batjes, N.H., 1996. Total carbon and nitrogen in the soils of the World. Eur. J. Soil Sci. 47, 151–163.

Bond-Lamberty, B., Thomson, A., 2010. Temperature-associated increases in the global soil respiration record. Nature 464, 579–582.

China Meteorological Administration, 2011. China Meteorological Data Daily Value. China Meteorological Data Sharing Service System, Beijing, China. http://cdc.cma.gov.cn/index.jsp.

Conant, R.T., Ryan, M.G., Ågren, G.I., Birge, H.E., Davidson, E.A., Eliasson, P.E., Evans, S.E., Frey, S.D., Giardina, C.P., Hopkins, F.M., Hyvönen, R., Kirschbaum, M.U.F., Lavallee, J.M., Leifeld, J., Parton, W.J., Steinweg, J.M., Wallenstein, M.D., Wetterstedt, J.Å.M., Bradford, M.A., 2011. Temperature and soil organic matter decomposition rates-synthesis of current knowledge and a way forward. Glob. Chang. Biol. 17, 3392–3404.

Davidson, E.A., Janssens, I.A., 2006. Temperature sensitivity of soil carbon decomposition and feedbacks to climate change. Nature 440, 165–173.

Dintwe, K., Okin, G.S., 2018. Soil organic carbon in savannas decreases with anthropogenic climate change. Geoderma 309, 7–16.

Enríquez-de-Salamanca, Á., Díaz-Sierra, R., Martín-Aranda, R.M., Santos, M.J., 2017. Environmental impacts of climate change adaptation. Environ. Impact Assess. Rev. 64, 87–96.

Francaviglia, R., Coleman, K., Whitmore, A.P., Doro, L., Urracci, G., Rubino, M., Ledd, L., 2012. Changes in soil organic carbon and climate change – application of the RothC model in agro-silvo-pastoral Mediterranean systems. Agric. Syst. 112, 48–54.

Gabarrón-Galeote, M.A., Trigalet, S., van Wesemael, B., 2015. Soil organic carbon evolution after land abandonment along a precipitation gradient in southern Spain. Agric. Ecosyst. Environ. 199, 114–123.

Gao, M.F., Qiu, J.J., Li, C.S., Wang, L.G., Li, H., Gao, C.Y., 2014. Modeling nitrogen loading from a watershed consisting of cropland and livestock farms in China using Manure-DNDC. Agric. Ecosyst. Environ. 185, 88–98.

Gaumont-Guay, D., Black, T.A., Griffis, T.J., Barr, A.G., Jassal, R.S., Nesic, Z., 2006. Interpreting the dependence of soil respiration on soil temperature and water content in a boreal aspen stand. Agric. For. Meteorol. 140, 220–235.

Gerten, D., Luo, Y.Q., Le Maire, G., Parton, W.J., Keough, C., Weng, E.S., Beier, C., Ciais, P., Cramer, W., Dukes, J.S., Hanson, P.J., Knapp, A.A.K., Linder, S., Nepstad, D., Rustad, L., Sowerby, A., 2008. Modelled effects of precipitation on ecosystem carbon and water dynamics in different climatic zones. Glob. Chang. Biol. 14, 2365–2379.

Ghosh, A., Bhattacharyya, R., Dwivedi, B.S., Meena, M.C., Agarwal, B.K., Mahapatra, P., Shahi, D.K., Salwani, R., Agnihorti, R., 2016. Temperature sensitivity of soil organic carbon decomposition as affected by long-term fertilization under a soybean based cropping system in a sub-tropical Alfisol. Agric. Ecosyst. Environ. 233, 202–213.

Gilhespy, S.L., Anthony, S., Cardenas, L., Chadwick, D., Prado, A.D., Li, C.S., Misselbrook, T., Rees, R.M., Salas, W., Sanz-Cobena, A., Smith, P., Tilston, E.L., Topp, C.F.E., Vetter, S., Yeluripati, J.B., 2014. First 20 years of DNDC (DeNitrification DeComposition): model evolution. Ecol. Model. 292, 51–62.

Goglio, P., Grant, B.B., Smith, W.N., Desjardins, R.L., Worth, D.E., Zentner, R., Malhi, S.S., 2014. Impact of management strategies on the global warming potential at the cropping system level. Sci. Total Environ. 490, 921–933.

Gollany, H.T., Elnaggar, A.A., 2017. Simulating soil organic carbon changes across toposequences under dryland agriculture using CQESTR. Ecol. Model. 355, 97–104.

Gottschalk, P., Smith, J.U., Wattenbach, M., Bellarby, J., Stehfest, E., Arnell, N., Osborn, T.J., Jones, C., Smith, P., 2012. How will organic carbon stocks in mineral soils evolve under future climate? Global projections using RothC for a range of climate change scenarios. Biogeosciences 9, 3151–3171.

Gray, J.M., Humphreys, G.S., Deckers, J.A., 2011. Distribution patterns of World Reference Base soil groups relative to soil forming factors. Geoderma 160, 373–383.

Grosz, B., Dechow, R., Gebbert, S., Hoffmann, H., Zhao, G., Constantin, J., Raynal, H., Wallach, D., Coucheney, E., Lewan, E., Eckersten, H., Specka, X., Kersebaum, K.C., Nendel, C., Kuhnert, M., Yeluripati, J., Haas, E., Teixeira, E., Bindi, M., Trombi, G., Moriondo, M., Doro, L., Roggero, P.P., Zhao, Z.G., Wang, E.L., Tao, F.L., Rötter, R., Kassie, B., Cammarano, D., Asseng, S., Weihermüller, L., Siebert, S., Gaiser, T., Ewert, F., 2017. The implication of input data aggregation on up-scaling soil organic carbon changes. Environ. Model. Softw. 96, 361–377.

Guntiñas, M.E., Gil-Sotres, F., Leirós, M.C., Trasar-Cepeda, C., 2013. Sensitivity of soil respiration to moisture and temperature. J. Soil Sci. Plant Nutr. 13, 445–461.

Huang, J., Ebach, M.C., Triantafilis, J., 2017. Cladistic analysis of Chinese Soil Taxonomy. Geoderma Reg. 10, 11–20.

Intergovernmental Panel on Climate Change, 2013. Climate Change 2013: Synthesis Report. Summary for Policymakers. Cambridge University Press, Cambridge, UK and New York, NY, USA.

Jenkinson, D.S., Rayner, J.H., 1977. The turnover of soil organic matter in some of Rothamsted classical experiments. Soil Sci. 125, 298–305.

Karhu, K., Auffret, M.D., Dungait, J.A., Hopkins, D.W., Prosser, J.I., Singh, B.K., Subke, J.A., Wookey, P.A., Ågren, G.I., Sebastià, M.T., Gouriveau, F., 2014. Temperature sensitivity of soil respiration rates enhanced by microbial community response. Nature 513, 81–84.

Kumar, S., 2015. Estimating spatial distribution of soil organic carbon for the Midwestern United States using historical database. Chemosphere 127, 49–57.

Labaz, B., Galka, B., Bogacz, A., Waroszewski, J., Kabala, C., 2014. Factors influencing humus forms and forest litter properties in the mid-mountains under temperate climate of southwestern Poland. Geoderma 230–231, 265–273.

Lal, R., 2004. Soil carbon sequestration to mitigate climate change. Geoderma 123, 1–22.

Leech, N.L., Barret, K.K.C., Morgan, G., 2008. SPSS for Intermediate Statistics. Lawrence Erlbaum Associates, New York, pp. 270.

Lefèvre, R., Barré, P., Moyano, F.E., Christensen, B.T., Bardoux, G., Eglin, T., Girardin, C., Houot, S., Kätterer, T., Oort, F.V., Chenu, C., 2014. Higher temperature sensitivity for stable than for labile soil organic carbon-evidence from incubations of long-term bare fallow soils. Glob. Chang. Biol. 20, 633–640.

Lei, H.J., Li, B.G., Bai, Y.L., Huang, Y.F., Lu, Y.Z., Li, G.T., 2006. Modeling soil organic matter dynamics under intensive cropping systems on the Huang-Huai-Hai plain of China. Pedosphere 16, 409–419.

Li, C.S., 2007a. Quantifying greenhouse gas emissions from soils: scientific basis and modeling approach. Soil Sci. Plant Nutr. 53, 344–352.

Li, C.S., 2007b. Quantifying soil organic carbon sequestration potential with modeling approach. In: Tang, H.J., Van Ranst, E., Qiu, J.J. (Eds.), Simulation of Soil Organic Carbon Storage and Changes in Agricultural Cropland in China and Its Impact on Food Security. China Meteorological Press, Beijing, pp. 1–14.

Li, C.S., Mosier, A., Wassmann, R., Cai, Z.C., Zheng, X.H., Huang, Y., Tsuruta, H., Boonjawat, J., Lantin, R., 2004. Modeling greenhouse gas emissions from rice-based production systems: sensitivity and upscaling. Glob. Biogeochem. Cycles 18, GB1043. https://doi.org/10.1029/2003GB002045.

Li, G.L., Kim, S.J., Park, M.J., Son, Y.H., 2017. Short-term effects of experimental warming and precipitation manipulation on soil microbial biomass C and N, community substrate utilization patterns and community composition. Pedosphere 27, 714–724.

Liao, Q.L., Zhang, X.H., Li, Z.P., Pan, G.X., Smith, P., Jin, Y., Wu, X.M., 2009. Increase in soil organic carbon stock over the last two decades in China's Jiangsu Province. Glob. Chang. Biol. 15, 861–875.

Liu, L.L., Wang, X., Lajeunesse, M.J., Miao, G.F., Piao, S.L., Wan, S.Q., Wu, Y.X., Wang, Z.H., Yang, S., Li, P., Deng, M.F., 2016. A cross-biome synthesis of soil respiration and its determinants under simulated precipitation changes. Glob. Chang. Biol. 22, 1394–1405.

Loague, K., Green, R.E., 1991. Statistical and graphical methods for evaluating solute transport models: overview and application. J. Contam. Hydrol. 7, 51–73.

Longbottom, T.L., Townsend-Small, A., Owen, L.A., Murari, M.K., 2014. Climatic and topographic controls on soil organic matter storage and dynamics in the Indian Himalaya: potential carbon cycle–climate change feedbacks. Catena 119, 124–135.

Luo, Z.K., Feng, W.T., Luo, Y.Q., Baldock, J., Wang, E.L., 2017. Soil organic carbon dynamics jointly controlled by climate, carbon inputs, soil properties and soil carbon fraction. Glob. Chang. Biol. 23, 4430–4439.

Meersmans, J., van Wesemael, B., Goidts, E., van Molle, M., De Baets, S., De Ridder, F., 2011. Spatial analysis of soil organic carbon evolution in Belgian croplands and grasslands, 1960–2006. Glob. Chang. Biol. 17, 466–479.

Meier, I.C., Leuschner, C., 2010. Variation of soil and biomass carbon pools in beech forests across a precipitation gradient. Glob. Chang. Biol. 16, 1035–1045.

Melillo, J.M., DeAngelis, K.M., Werner, W.J., Bernard, M.J., Bowles, F.P., Pold, G., Knorr, M.A., Grandy, A.S., 2017. Long-term pattern and magnitude of soil carbon feedback to the climate system in a warming world. Science 358, 101–105.

Muñoz-Rojas, M., Abd-Elmabod, S.K., Zavala, L.M., De la Rosa, D., Jordán, A., 2017. Climate change impacts on soil organic carbon stocks of Mediterranean agricultural areas: a case study in Northern Egypt. Agric. Ecosyst. Environ. 238, 142–152.

Mureva, A., Ward, D., 2017. Soil microbial biomass and functional diversity in shrub-encroached grasslands along a precipitation gradient. Pedobiologia 63, 37–45.

Pacey, J.G., DeGier, J.P., 1986. The factors influencing landfill gas production. In: Energy From Landfill Gas. Proceeding of a Conference Jointly Sponsored by the United Kingdom Department of Energy and the United States Department of Energy (October 1986), pp. 51–59.

Pan, G.X., Xu, X.W., Smith, P., Pan, W.N., Lal, R., 2010. An increase in topsoil SOC stock of China's croplands between 1985 and 2006 revealed by soil monitoring. Agric. Ecosyst. Environ. 136, 133–138.

Pathak, H., Li, C.S., Wassmann, R., 2005. Greenhouse gas emissions from Indian rice fields: calibration and upscaling using the DNDC model. Biogeosciences 2, 113–123.

Peinetti, H.R., Menezes, R.S.C., Tiessen, H., Marin, A.M.P., 2008. Simulating plant productivity under different organic fertilization practices in a maize/native pasture rotation system in semi-arid NE Brazil. Comput. Electron. Agric. 62, 204–222.

Poll, C., Marhan, S., Back, F., Niklaus, P.A., Kandeler, E., 2013. Field-scale manipulation of soil temperature and precipitation change soil CO_2 flux in a temperate agricultural ecosystem. Agric. Ecosyst. Environ. 165, 88–97.

Qi, R.M., Li, J., Lin, Z.A., Li, Z.J., Li, Y.T., Yang, X.D., Zhang, J.J., Zhao, B.Q., 2016. Temperature effects on soil organic carbon, soil labile organic carbon fractions, and soil enzyme activities under long-term fertilization regimes. Appl. Soil Ecol. 102, 36–45.

Royles, J., Amesbury, M.J., Convey, P., Griffiths, H., Hodgson, D.A., Leng, M.J., Charman, D.J., 2013. Plants and soil microbes respond to recent warming on the Antarctic Peninsula. Curr. Biol. 23, 1702–1706.

Saint-Laurent, D., Gervais-Beaulac, V., Berthelot, J.S., 2014. Variability of soil properties in different flood-risk zones and link with hydroclimatic changes (Southern Québec, Canada). Geoderma 214–215, 80–90.

Sakurai, G., Jomura, M., Yonemura, S., Iizumi, T., Shirato, Y., Yokozawa, M., 2012. Inversely estimating temperature sensitivity of soil carbon decomposition by assimilating a turnover model and long-term field data. Soil Biol. Biochem. 46, 191–199.

Sardans, J., Peñelas, J., Estiarte, M., Prieto, P., 2008. Warming and drought alter C and N concentration, allocation and accumulation in a Mediterranean shrubland. Glob. Chang. Biol. 14, 2304–2316.

Schimel, D.S., Braswell, B.H., Holland, E.A., McKeon, R., Ojima, D.S., Painter, T.H., Parton, W.J., Townsend, A.R., 1994. Climatic, edaphic, and biotic controls over storage and turnover of carbon in soils. Glob. Biogeochem. Cycles 8 (3), 279–293.

Shahid, M., Nayak, A.K., Puree, C., Tripathi, R., Lal, B., Gautam, P., Bhattacharyya, P., Mohanty, S., Kumar, A., Panda, B.B., Kumar, U., Shukla, A.K., 2017. Carbon and nitrogen fractions and stocks under 41 years of chemical and organic fertilization in a sub-humid tropical rice soil. Soil Tillage Res. 170, 136–146.

Shi, X.Z., Yang, R.W., Weindorf, D.C., Wang, H.J., Yu, D.S., Huang, Y., Pan, X.Z., Sun, W.X., Zhang, L.M., 2010. Simulation of organic carbon dynamics at regional scale for paddy soils in China. Clim. Chang. 102, 579–593.

Singh, B.R., Lal, R., 2005. The potential of soil carbon sequestration through improved management practices in Norway. Environ. Dev. Sustain. 7, 161–184.

Singh, S.K., Pandey, C.B., Sidhu, G.S., Sarkar, D., Sagar, R., 2011. Concentration and stock of carbon in the soils affected by land uses and climates in the western Himalaya, India. Catena 87, 78–89.

Six, J., Conant, R.T., Paul, E.A., Paustian, K., 2002. Stabilization mechanisms of soil organic matter: implications for C saturation of soils. Plant Soil 241, 155–176.

Smit, B., Skinner, M.W., 2002. Adaptation options in agriculture to climate change: a typology. Mitig. Adapt. Strateg. Glob. Chang. 7, 85–114.

Smith, P., Smith, J.U., Powlson, D.S., McGill, W.B., Arah, J.R.M., Chertov, O.G., Coleman, K., Franko, U., Frolking, S., Jenkinson, D.S., Jensen, L.S., Kelly, R.H., Gunnewiek, H.K., Komarov, A.S., Li, C.S., Molina, J.A.E., Mueller, T., Parton, W.J., Thornley, J.H.M., Whitmore, A.P., 1997. A comparison of the performance of nine soil organic matter models using datasets from seven long term experiments. Geoderma 81, 153–225.

Streit, K., Hagedorn, F., Hiltbrunner, D., Portmann, M., Saurer, M., Buchmann, N., Wild, B., Richter, A., Wipf, S., Siegwolf, R.T.W., 2014. Soil warming alters microbial substrate use in alpine soils. Glob. Chang. Biol. 20, 1327–1338.

Tang, H.J., Qiu, J.J., Van Ranst, E., Li, C.S., 2006. Estimations of soil organic carbon storage in cropland of China based on DNDC model. Geoderma 134, 200–206.

Tonitto, C., David, M.B., Drinkwater, L.E., Li, C.S., 2007. Application of the DNDC model to tile-drained Illinois agroecosystems: model calibration, validation, and uncertainty analysis. Nutr. Cycl. Agroecosyst. 78, 51–63.

Wang, L.G., Qiu, J.J., Tang, H.J., Li, H., Li, C.S., Van Ranst, E., 2008. Modelling soil organic carbon dynamics in the major agricultural regions of China. Geoderma 147, 47–55.

Whitmore, A.P., Klein-Gunnewiek, H., Crocker, G.J., Klir, J., Körschens, M., Poulton, P.R., 1997. Simulating trends in soil organic carbon in long-term experiments using the Verberne/MOTOR model. Geoderma 81, 137–151.

Wu, Z.T., Dijkstra, P., Koch, G.W., Peñuelas, J., Hungate, B.A., 2011. Responses of terrestrial ecosystems to temperature and precipitation change: a meta-analysis of experimental manipulation. Glob. Chang. Biol. 17, 927–942.

Xie, Z.B., Zhu, J.G., Liu, G., Cadisch, G., Hasegawa, T., Chen, C.M., Sun, H.F., Tang, H.Y., Zeng, Q., 2007. Soil organic carbon stocks in China and changes from 1980s to 2000s. Glob. Chang. Biol. 13, 1989–2007.

Xu, S.X., Shi, X.Z., Zhao, Y.C., Yu, D.S., Li, C.S., Wang, S.H., Tan, M.Z., Sun, W.X., 2011. Carbon sequestration potential of recommended management practices for paddy soils of China, 1980–2050. Geoderma 166, 206–213.

Yang, Y.L., Shi, X.Z., Wang, G., Yu, D.S., Xu, M., Wang, H.J., 2009. Spatial heterogeneity of soil properties and their affecting factors in the Northern Jiangsu Province. Chin. J. Soil Sci. 40, 465–470 (in Chinese with English abstract).

Yang, Y.H., Luo, Y.Q., Finzi, A.C., 2011. Carbon and nitrogen dynamics during forest stand development: a global synthesis. New Phytol. 190, 977–989.

Yu, Y.Y., Guo, Z.T., Wu, H.B., 2006. Changes in organic carbon of cultivated soils in China from 1980 to 2000. Mar. Geol. Quat. Geol. 26, 123–130 (in Chinese with English abstract).

Yu, Y.Q., Huang, Y., Zhang, W., 2013. Projected changes in soil organic carbon stocks of China's croplands under different agricultural managements, 2011–2050. Agric. Ecosyst. Environ. 178, 109–120.

Zhang, L.M., Yu, D.S., Shi, X.Z., Xu, S.X., Xing, S.H., Zhao, Y.C., 2014. Effects of soil data and simulation unit resolution on quantifying changes of soil organic carbon at regional scale with a biogeochemical process model. PLoS One 9 (2), e88622. https://doi.org/10.1371/journal.pone.0088622.

Zhang, K.R., Dang, H.S., Zhang, Q.F., Cheng, X.L., 2015. Soil carbon dynamics following land-use change varied with temperature and precipitation gradients: evidence from stable isotopes. Glob. Chang. Biol. 21, 2762–2772.

Zhang, L.M., Zhuang, Q.L., Li, X.D., Zhao, Q.Y., Yu, D.S., Liu, Y.L., Shi, X.Z., Xing, S.H., Wang, G.X., 2016. Carbon sequestration in the uplands of Eastern China: an analysis with high-resolution model simulations. Soil Tillage Res. 158, 165–176.

Zhang, L.M., Liu, Y.L., Li, X.D., Huang, L.B., Yu, D.S., Shi, X.Z., Chen, H.Y., Xing, S.H., 2018. Effects of soil map scales on simulating soil organic carbon changes of upland soils in Eastern China. Geoderma 312, 159–169.

Zhao, Y.C., Shi, X.Z., Weindorf, D.C., Yu, D.S., Sun, W.X., Wang, H.J., 2006. Map scale effects on soil organic carbon stock estimation in North China. Soil Sci. Soc. Am. J. 70, 1377–1386.

Zhao, G., Bryan, B.A., King, D., Luo, Z.K., Wang, E.L., Song, X.D., Yu, Q., 2013. Impact of agricultural management practices on soil organic carbon: simulation of Australian wheat systems. Glob. Chang. Biol. 19, 1585–1597.

Zhao, J.X., Luo, T.X., Li, R.C., Wei, H.X., Li, X., Du, M.Y., Tang, Y.H., 2018. Precipitation alters temperature effects on ecosystem respiration in Tibetan alpine meadows. Agric. For. Meteorol. 252, 121–129.

Zhi, J.J., Jing, C.W., Lin, S.P., Zhang, C., Cao, Z., Liu, Q.K., DeGloria, S.D., Wu, J.P., 2014. Estimating soil organic carbon stocks and spatial patterns with statistical and GIS-based methods. PLoS One 9 (5), e97757. https://doi.org/10.1371/journal.pone.0097757.

Zhou, X.H., Wang, E.S., Luo, Y.Q., 2008. Modeling patterns of nonlinearity in ecosystem responses to temperature, CO_2, and precipitation change. Ecol. Appl. 18, 453–466.

Zou, J.L., Tobin, B., Luo, Y.Q., Osborne, B., 2018. Response of soil respiration and its components to experimental warming and water addition in a temperate Sitka spruce forest ecosystem. Agric. For. Meteorol. 260–261, 204–215.